Talanta 84 (2011) 400–405

Contents lists available at ScienceDirect

Talanta

journal homepage: www.elsevier.com/locate/talanta

A sensitive enzymatic method for paraoxon detection based on enzyme inhibition and fluorescence quenching

Kuikui Wang[c], Lei Wang[b,**], Wei Jiang[a,*], Jingtian Hu[c]

[a] School of Chemistry and Chemical Engineering, Shandong University, 250100 Jinan, PR China
[b] School of Pharmacy, Shandong University, 250012 Jinan, PR China
[c] Environment Research Institute, Shandong University, 250100 Jinan, PR China

ARTICLE INFO

Article history:
Received 6 November 2010
Received in revised form 6 January 2011
Accepted 16 January 2011
Available online 26 January 2011

Keywords:
Acetylcholinesterase
Paraoxon
Fluorescence
Quantitative detection

ABSTRACT

A sensitive and selective method for the paraoxon detection based on enzyme inhibition and fluorescence quenching was presented in this study. Under the catalytic effect of acetylcholinesterase (AChE), acetylthiocholine (ATCh) hydrolysis released thiocholine (TCh) which could react with N-(7-dimethylamino-4-methylcoumarin-3-yl) maleimide (DACM) to produce a blue fluorescence compound. Subsequently, AChE catalytic activity was inhibited with the addition of paraoxon, which caused TCh decreased, leading to a significant decrease of the blue fluorescent compound. Meanwhile, p-nitrophenol, the hydrolysis product of paraoxon, would lead to a quenching of the fluorescence. Therefore, fluorescence intensity of the system would decrease dramatically by a combined effect of enzyme inhibition and fluorescence quenching. Under optimal experimental conditions, an excellent linear relationship between the decrease of fluorescence intensity and paraoxon concentration over the range from 5.5×10^{-12} to 1.8×10^{-10} mol L^{-1} was obtained. Fluorescence background caused by nonenzymatic hydrolysis of ATCh or other matters was relatively low, the proposed approach offered adequate sensitivity for the detection of paraoxon at 3.5×10^{-12} mol L^{-1}.

© 2011 Elsevier B.V. All rights reserved.

1. Introduction

Organophosphorus compounds (OP) have been widely used as pesticides and chemical warfare agents [1,2]. They are toxic to mammals, especially when ingested, inhaled, or absorbed through the skin. As a matter of fact, OP compounds are irreversible inhibitors of well-known esterase phosphorylation in the central nerve system. The primary enzyme inhibited by OP compounds is the acetylcholinesterase (AChE) [3,4]. AChE can catalyze the hydrolysis of acetylcholine (ACh), when the AChE activity is inhibited, the accumulation of ACh results in transmitting nerve impulses frustration, leading to serious health problems or even ultimately death [5,6]. Paraoxon is a typical OP compound, which can inhibit the AChE activity [7,8].

Numerous analytical methods have been used for the detection of OP compounds [9], including gas chromatography–mass spectrum (GC–MS) [10], high performance liquid chromatography (HPLC) [11–13], electrochemical method [14,15] and immunoassay [16,17]. GC–MS, HPLC and electrical techniques are all sensitive and reliable methods, however, they are time-consuming and expensive. Immunoassay is an effective method with high sensitivity, selectivity and reproducibility, but it needs corresponding antibody [17,18]. It is believed that enzymatic bioassay has the ability to overcome these problems [19]. Leblanc and co-workers used enzymatic bioassay to detect paraoxon and achieved a detection limit of 5×10^{-9} mol L^{-1} [20].

AChE can also catalyze the hydrolysis of acetylthiocholine (ATCh), and produce thiocholine (TCh). By binding to OP compounds, AChE is irreversibly inhibited and forms the phosphorylated and unreactive enzyme. It can be utilized in bioassay if AChE can present the qualitative or quantitative data regarding to the hydrolysis reaction of OP compounds [21,22]. Liu and Lin self-assembled AChE on carbon nanotubes and detected paraoxon on the basis of enzyme inhibition, obtained a comparable result which was similar to that obtained with BChE biosensors [23]. Arduini et al. quantified anticholinesterase pesticides based on the lost enzymatic activity measurement after exposure to OP compounds [24]. Both results demonstrated an easiness of preparation together with high sensitivity and potentialities for pesticide measurement.

Fluorescent probes are often utilized to detect low concentrations of single analyte and individual component of complex systems, which display good sensitivity and selectivity [25]. Upon photoexcitation, coumarin derivatives display high fluorescence quantum yield in the blue-green region. The fluorescence

* Corresponding author. Tel.: +86 531 88363888; fax: +86 531 88564464.
** Corresponding author. Tel.: +86 531 88382330.
E-mail addresses: wangl-sdu@sdu.edu.cn (L. Wang), wjiang@sdu.edu.cn (W. Jiang).

0039-9140/$ – see front matter © 2011 Elsevier B.V. All rights reserved.
doi:10.1016/j.talanta.2011.01.056

properties of coumarin derivatives could be used to investigate enzymatic process [26]. N-(7-dimethylamino-4-methylcoumarin-3-yl) maleimide (DACM) is a thiol reactive dialkylcoumarin, which can produce intensive blue-fluorescence compounds when it reacts with sulfhydryl compounds. Fluorescence emission of the DACM conjugates is moderately sensitive to environment [27–29]. In addition, the emission spectrum of DACM (477 nm) can overlap with the absorbance spectrum of the p-nitrophenol (pNP, 400 nm), which would lead to fluorescence resonance energy transfer (FRET) and quench the coumarin emission [30]. In a recent study, FRET between pNP and coumarin was utilized for the detection of low concentrations of paraoxon [25].

On the basis of enzyme inhibition and fluorescence quenching, a sensitive method for the paraoxon detection was presented here. Briefly, the study was achieved via two step fluorescence decrease. The first step was attributed to the effect of paraoxon which could irreversibly inhibit the catalytic activity of AChE, leading to the blue fluorescent compound decreasing accordingly; the second step was attributed to the effect of pNP which could cause FRET phenomenon, leading to a fluorescence quenching. Under the dual effects of enzyme inhibition and fluorescence quenching, paraoxon was detected without separating from the solution and the detection limit was 3.5×10^{-12} mol L^{-1}.

2. Experimental

2.1. Reagents and materials

The acetylcholinesterase (AChE, from electrophorus electricus) and acetylthiocholine chloride (ATCh) were purchased from Sigma–Aldrich. DACM was purchased from Anaspec. Paraoxon (100 mg L^{-1}, acetone solution) was purchased from China Standard Technology Development Corporation.

PBS buffer solution (pH 8.5, 1.0×10^{-2} mol L^{-1}) was prepared by dissolving 3.4 g $Na_2HPO_4 \cdot 12H_2O$ (99.0%), 8.0×10^{-2} g $NaH_2PO_4 \cdot 2H_2O$ (99.0%) and 0.85 g NaCl (99.5%) and then diluting to 100 mL with water.

Tris–HCl buffer solution (pH 7.5, 2.0×10^{-2} mol L^{-1}) was prepared by dissolving 0.24 g Tris (trihydroxymethyl aminomethane) (99.5%) in 100 mL water and then adjusting pH to 7.5 with HCl.

All other chemicals were of analytical grade and the solvents were purified using a MilliQ apparatus.

2.2. Apparatus

All the fluorescence measurements were performed on a Hitachi F-4500 spectrofluorimeter (Hitachi, Japan).

All absorption spectra were measured on a UV-2500PC spectrophotometer (Shimadzu, Japan).

The pH was measured on a Lei Ci PHS-3C pH-meter (Shanghai, China).

2.3. Methods

Paraoxon solutions were diluted with the PBS buffer (pH 8.5) and mixed in the Tris–HCl buffer (pH 7.5) to AChE solution of 9.0×10^{-10} mol L^{-1} and paraoxon of 2.0×10^{-10} mol L^{-1}. The mixture was incubated at 37 °C for 60 min. Then ATCh and DACM were added to a level of 7.4×10^{-7} mol L^{-1} and 4.5×10^{-6} mol L^{-1}, subsequently incubated for 60 min at 37 °C. Fluorescence spectra were measured with excitation and emission slit width of 10 nm. The emission spectra were obtained by setting the excitation wavelength at 390 nm and recording the emission wavelength from 420 nm to 600 nm.

The fluorescence spectra of the blank solutions were measured under the same conditions.

3. Results and discussion

3.1. The fluorescence spectra and UV–visible absorption spectra of the system

The fluorescence properties of different solutions were studied to observe the enzyme inhibition of paraoxon and fluorescence quenching of pNP. Fig. 1 illustrated the reaction scheme of the process, which was briefly described as follows. Firstly, the hydrolysis of ATCh by AChE, acetate and TCh were produced. Then a blue fluorescence product was formed as a result of the reaction of TCh and DACM. Enzymatic activity was inhibited and pNP was formed with the addition of paraoxon [24]. The product (pNP) would lead to fluorescence quenching of the compound TCh-DACM, resulting in a further fluorescence decrease of the fluorescence system [25].

To verify the occurrence of enzyme inhibition and fluorescence quenching effects in the system, the fluorescence spectra different systems were studied. Fig. 2 showed the fluorescence spectra of different systems. Curve 1, 2 and 3 were the fluorescence spectra of DACM, ATCh-DACM and AChE-DACM, respectively. When the system only included DACM, ATCh-DACM or AChE-DACM, the fluorescence intensity was low, which showed low fluorescence background [27]. Curve 4 and curve 6 corresponded to the fluorescence spectra of AChE-ATCh-DACM and AChE-paraoxon-ATCh-DACM, respectively. The respective chemicals in different systems were at same concentrations. As illustrated in Fig. 2, when AChE, ATCh and DACM existed together, the intense fluorescence signal was generated. By comparing curve 4 with DACM, ATCh-DACM and AChE-DACM systems (curve 1, 2 and 3), it was obvious that the intense fluorescence signal was produced due to the reaction between TCh (hydrolysis product of ATCh) and DACM. However, compared with curve 4, the fluorescence signal of curve 6 was weaken when paraoxon was added into the system. The result indicated that the addition of paraoxon led to the fluorescence signal decrease, which was a direct proof that enzyme inhibition occurred in the AChE-paraoxon-ATCh-DACM system [24].

Curve 5 was the fluorescence spectrum of AChE-ATCh-DACM-pNP system. By comparison with curve 4 (AChE-ATCh-DACM system), it was found that, at an adding dosage of 1.5×10^{-10} mol L^{-1} pNP, the fluorescence intensity decreased. The concentrations of paraoxon and AChE were 2.0×10^{-10} mol L^{-1} and 9.0×10^{-10} mol L^{-1}, which could produce $\sim 10^{-10}$ mol L^{-1} pNP, so 1.5×10^{-10} mol L^{-1} was chosen for pNP. That demonstrated pNP could lead to the fluorescence signal quenching [25]. However, the fluorescence intensity of curve 5 was higher than curve 6 (AChE-paraoxon-ATCh-DACM system). The relative decrease in the fluorescence intensity at the second effect of fluorescence quenching by pNP was less than that obtained at the first effect of enzyme inhibition by paraoxon. It was concluded that both paraoxon and pNP could make fluorescence signal decreased, and the main effect was caused by paraoxon. As mentioned above, the fluorescence quenching would play a role in fluorescence decrease after enzyme inhibition effect. Therefore, after paraoxon inhibiting enzyme activity and producing pNP, pNP could lead to a larger quenching in the determination.

Further studies are required to confirm that both enzyme inhibition and fluorescence quenching effect occurred in studied system. UV–visible absorption spectra of AChE solutions were measured in paraoxon solutions at different concentrations (Fig. 3). Fig. 3 showed spectrum of the paraoxon (curve 1) in aqueous solution with an absorption band situated at 274 nm characteristic of the single component paraoxon. Spectra 2 and 3 corresponded to the absorption of paraoxon-AChE system with different AChE concentrations of 6.0×10^{-8} mol L^{-1} and 1.2×10^{-7} mol L^{-1}, respectively. There was only an absorption peak of paraoxon present (curve 1), and a new band situated at 400 nm was observed when AChE was

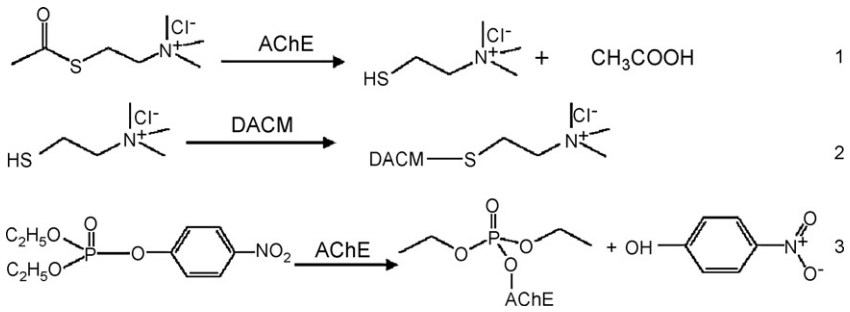

Fig. 1. Schematic illustration of the process: (A) ATCh hydrolysis by AChE, (B) TCh labeling with DACM, (C) paraoxon reacting with AChE.

added into paraoxon solution (curve 2 and 3). As shown in Fig. 3, the decrease of paraoxon absorption was paralleled by an increase of the new absorption as AChE concentrations increasing. Curve 4 was the absorption spectrum of pNP, and the absorption maximum of pNP was at 400 nm, which demonstrated the new products of curve 2 and 3 were pNP. The symmetry between the decrease in absorbance at 274 nm and the increase in absorbance at 400 nm was also a direct proof that paraoxon reacted with the AChE. It was demonstrated that a similar amount of pNP was produced. As illustrated from the spectra, no other effects were involved in the reaction process.

An isosbestic point at 307 nm was observed in Fig. 3, which suggested the coexistence of paraoxon and pNP, and no other intermediates were involved in the reaction. The effect of the isosbestic point demonstrated the total concentration of paraoxon and pNP was a constant [20]. And it was also observed that when paraoxon concentration was decreased, there was an increase in pNP concentration. Furthermore, the molar absorptivity of paraoxon and pNP was balanced at 307 nm. It was concluded that paraoxon could lead to enzyme inhibition and the reaction of paraoxon with AChE produced pNP, which would be detected by the fluorescence method.

3.2. Effect of DACM concentration

DACM was employed to generate intensive fluorescence signal with TCh in this study. The reaction between DACM and TCh was an irreversible interaction with rapid binding kinetics, which would produce stable DACM-TCh complex [26]. In order to get the intense and stable fluorescence signal, the effect of different DACM concentrations from 4.5×10^{-7} mol L^{-1} to 9.0×10^{-6} mol L^{-1} was studied. DACM concentration was investigated using $\Delta F = (F_1 - F_0)$ as standard. F_1 and F_0 were the fluorescence intensity of the system when paraoxon was absent and present, respectively. Hence, ΔF could display the effect of DACM concentration on the fluorescent system. As shown in Fig. S1 in Supporting Information, ΔF increased with the DACM concentration below 3.3×10^{-6} mol L^{-1} and changed little from 3.3×10^{-6} mol L^{-1} to 6.0×10^{-6} mol L^{-1}. However, ΔF decreased with the concentration above 6.0×10^{-6} mol L^{-1}. A possible reason was that, when lower than 3.3×10^{-6} mol L^{-1}, DACM was not enough to react with all TCh. When DACM concentration was up to 3.3×10^{-6} mol L^{-1}, all TCh was saturated with the DACM, and any more DACM added to the solution could not affect ΔF. Therefore, ΔF was kept relatively stable. Finally, a DACM concentration of 5.0×10^{-6} mol L^{-1} was selected in this assay. The effect of the DACM concentration on ΔF could further prove that the changes of the fluorescence signal were due to the combination of TCh and DACM.

3.3. Effect of pH

For the fluorescence intensity of analysis system and the activity of free enzyme, the pH profiles share the similar trend [31]. There was no obvious pH change during the experiment process, which demonstrated that the observed pH dependence of the sensor response was due to the pH dependence of the enzyme activity and TCh-DACM conjunction. The best pH condition for AChE enzyme

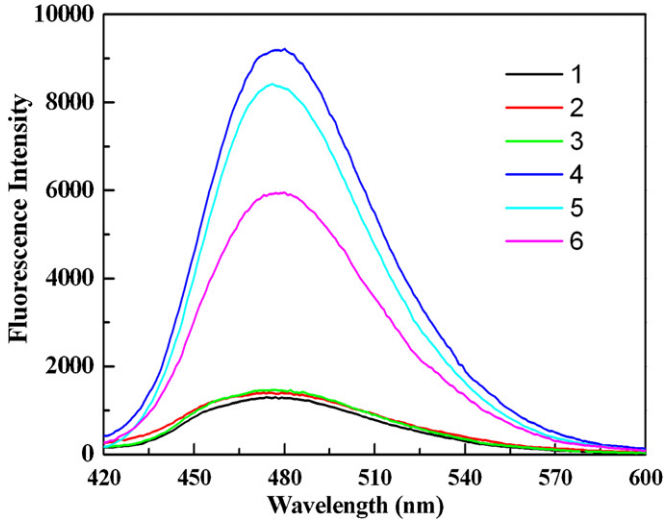

Fig. 2. Fluorescence spectra of the system: (1) DACM, (2) ATCh-DACM, (3) AChE-DACM, (4) AChE-ATCh-DACM, (5) AChE-ATCh-DACM-pNP, (6) AChE-paraoxon-ATCh-DACM. The concentrations of AChE, ATCh, DACM, paraoxon and pNP were 9.0×10^{-10} mol L^{-1}, 7.4×10^{-7} mol L^{-1}, 4.5×10^{-6} mol L^{-1}, 2.0×10^{-10} mol L^{-1} and 1.5×10^{-10} mol L^{-1}, pH 8.5.

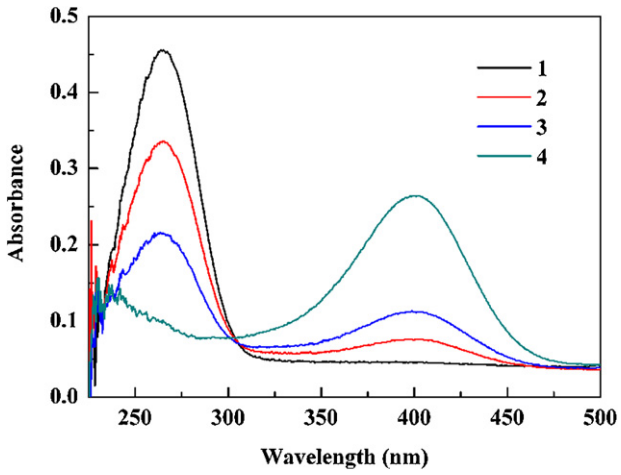

Fig. 3. UV–visible absorption spectra of the different systems. (1) Paraoxon 6.0×10^{-7} mol L^{-1}, (2) paraoxon 6.0×10^{-7} mol L^{-1}-AChE 6.0×10^{-8} mol L^{-1}, (3) paraoxon 6.0×10^{-7} mol L^{-1}-AChE 1.2×10^{-7} mol L^{-1}, (4) pNP 1.7×10^{-7} mol L^{-1}, pH 8.5.

catalysis is close to 8.0 [32], and DACM is more stable in the alkaline environment or else it would decompose. The optimal reacting condition for DACM with sulfhydryl groups was also in alkaline environment [33], so the pH value was optimized from 7.0 to 11. As shown in Fig. S2 in Supporting Information, the optimal pH condition was between 8.0 and 9.0. The possible reason was that, as the pH value increased from 7.0 to 8.5, the enzyme activity raised and DACM was more stable to react with TCh, leading to the increasing fluorescence intensity. However, the enzyme activity decreased as the pH value continued to increase to more than 8.5. The fluorescence intensity reached the maximum and more stable during this range, therefore, pH 8.5 was chosen in the study.

3.4. Effect of reaction time of paraoxon and AChE

The reaction time between paraoxon and AChE was also a factor influencing the fluorescence intensity of systems, experiments suggested that time plays an important role in the enzyme inhibition effect and fluorescence quenching effect [23,24]. Therefore, the effect of different paraoxon incubation time on ΔF was also studied under optimal conditions as mentioned above. As shown in Fig. S3 in Supporting Information, fluorescence signal increased with the increase of reaction time within 60 min, but the signal remained invariant when reaction time was longer than 60 min. The possible reason was that, as the time increased within 60 min, the inhibition effect strengthened and the generating pNP increased, leading to the enhancement of the quenching effect. The reaction time required 60–90 min to acquire the best result, therefore, fluorescence intensity was maintained at a stable level. After 90 min, AChE activity was almost inhibited completely and the free remainder of AChE was inactivated as the increase of time, so there was no need to study after 90 min. Finally, 75 min was chosen for reaction time in the assay.

3.5. Effect of interfering substances

Two different experiments were carried out to evaluate the possible interference effect due to the common presence of substances in the sample. In the first experiment, 1.0×10^{-10} mol L^{-1} paraoxon was added into AChE solution, after the incubation time, ATCh and DACM were added to measure the fluorescence intensity. In a second experiment, in the other hand, the substrate was added into the same paraoxon containing the interference specie which belonging to different groups, such as inorganic ions, detergents, organic pesticides, PCB, nitrophenol, carbon compounds and organic acids. In this case, concentrations used for different groups are those reported as the maximum admissible value for wastewater [34].

In the change of relative fluorescence intensity (ΔF%), a relative error of ±5.0% was considered to be tolerable. As shown in Table 1, various common salts such as NaCl, $CuSO_4$, $ZnSO_4$, $Cd(NO_3)_3$, NaF and $Ca(NO_3)_2$ are allowed to be present at high tolerable molar ratios (>10^5). The similar result was also observed for glucose, galactose, sodium acetate, sodium citrate and glycerol with the tolerable molar ratios >10^4. The influences of organic chlorine pesticide (dicofol and lindane) and organic fluorine pesticide (fluoroacetamide) were studied, which was observed that the tolerable molar ratios for these possible interferents were higher than 100.

The tolerances to 2,2′,5,5′-tetrachlorobenzidine and 2,4,4′-trichlorobiphenyl were higher, 2-nitrophenol and 3-nitrophenol were also tested that the tolerable molar ratios were higher than 700. However, detergents were tested as possible interfering specie as shown in Table 1, because both trictylphosphine oxide (TOPO) and sodium dodecyl sulfate (SDS) could influence enzymatic activity.

Table 1
Effects of conceivable interference on the determination of paraoxon (1.0×10^{-10} mol L^{-1}).

Substances	Tolerable concentration (mol L^{-1})	Molar ratio	ΔF%
NaCl	1.0×10^{-3}	10^7	−1.3
$CuSO_4$	1.0×10^{-5}	10^5	1.8
$ZnSO_4$	1.0×10^{-5}	10^5	−1.2
$Cd(NO_3)_3$	1.0×10^{-5}	10^5	−1.6
NaF	1.0×10^{-5}	10^5	0.9
$Ca(NO_3)_2$	1.0×10^{-5}	10^5	0.7
Glucose	1.0×10^{-6}	10^4	−2.4
Galactose	1.0×10^{-6}	10^4	−2.7
Sodium acetate	1.0×10^{-6}	10^4	4.2
Sodium citrate	1.0×10^{-6}	10^4	2.2
Glycerol	1.0×10^{-6}	10^4	−1.9
Dicofol	1.0×10^{-8}	100	−5.0
Lindane	1.0×10^{-8}	100	−4.9
Fluoroacetamide	2.0×10^{-8}	200	4.9
2,4,4′-trichlorobiphenyl	4.0×10^{-8}	400	−4.9
2,2′,5,5′-tetrachlorobenzidine	5.0×10^{-8}	500	4.9
2-nitrophenol	7.0×10^{-8}	700	−4.9
3-nitrophenol	1.0×10^{-7}	1000	−4.8
Trictylphosphine oxide (TOPO)	5.0×10^{-9}	50	−4.6
Sodium dodecyl sulfate (SDS)	6.0×10^{-9}	60	−4.7

It was found that there was little interference from commonly existed substances of different groups except detergents. Thus, the new sensitive fluorometric method displays high selectivity for the determination of paraoxon.

3.6. Calibration curve and detection limit

Under optimized conditions described above, it was found that the fluorescence system produced sensitive and selective responses to varying paraoxon concentrations. Over the concentration range from 5.5×10^{-12} mol L^{-1} to 1.8×10^{-10} mol L^{-1}, an excellent linear relationship between ΔF and paraoxon concentration was observed in Fig. 4. The linear regression equation was determined to be $Y = 8.70 \times 10^3 - 1.31 \times 10^{13}\ X$ ($r = 0.9974$). The detection limit of this assay was 3.5×10^{-12} mol L^{-1}, which was 2–3 orders of magnitude lower than that were observed in conventional methods [16,35]. In summary, these results provide evidence that this detection method can work well for paraoxon determination. More importantly, the detection limit is comparable to or better than the values for other AChE inhibition-based biosensors [20,25]. This

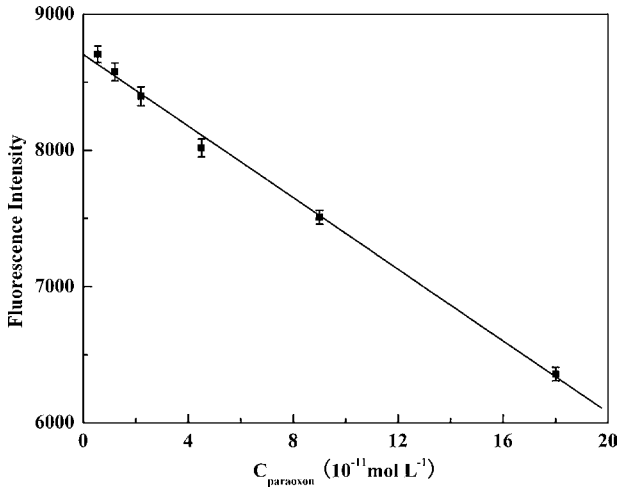

Fig. 4. Linear relationship between fluorescence intensity and the concentration of paraoxon. The concentrations of AChE, ATCh and DACM were 9.0×10^{-10} mol L^{-1}, 7.4×10^{-7} mol L^{-1} and 4.5×10^{-6} mol L^{-1}, pH 8.5.

Table 2
Recovery studies of spiked practical water samples ($n = 5$).

Sample	Added (10^{-11} mol L^{-1})	Found (10^{-11} mol L^{-1})	Recovery (%)	R.S.D. (%)
Tap water 1	1.5	1.4	93.7	2.2
	3.0	3.1	103.3	2.5
	6.0	6.5	108.3	3.2
Tap water 2	1.5	1.6	106.7	0.6
	3.0	3.3	110.0	1.0
	6.0	6.1	101.7	1.4
Lake water 1	3.0	2.9	103.5	1.3
	6.0	5.7	95.0	2.5
	9.0	8.7	96.7	3.1
Lake water 2	3.0	3.1	103.3	1.6
	6.0	5.7	97.0	2.3
	9.0	9.5	105.6	2.8

should make the biosensor an ideal analytical tool for sensitive detection of organophosphates in the environment without any sample preconcentration.

3.7. Sample analyses and the recovery

To monitor the accuracy of an analytical method, spike recovery is a useful tool. Recovery less than 100% indicates the measured values for a matrix are lower than the nominal value of the spike, otherwise higher than the nominal value of the spike [36]. The variability was low if there were no interferences or matrix effects, so a recovery close to 100% was expected.

Four samples, two tap water samples and the other two water samples from natural lakes, were filtered through a 0.22 μm membrane and the pH was adjusted to 8.5. After simple pretreatment, different concentrations of paraoxon were added to study the recovery under the optimal conditions.

The average recovery of the experiments at each level must be in the range of 70–120%, with a variation coefficient of ±20% to fulfill the standards [34]. In this study, about 1.5×10^{-11} mol L^{-1}, 3.0×10^{-11} mol L^{-1} and 6.0×10^{-11} mol L^{-1} paraoxon were added into tap water samples, 3.0×10^{-11} mol L^{-1}, 6.0×10^{-11} mol L^{-1} and 9.0×10^{-11} mol L^{-1} paraoxon were added into lake water samples. Table 2 showed the results obtained by analysis of these spiked samples. The recoveries of tap water 1, 2 and lake water 1, 2 were observed in the range of 93.7–108.3%, which demonstrated low matrix effect on the fluorescence signal. The low relative standard deviations for paraoxon demonstrated the high precision of analysis. Additionally, a very low relative standard deviation of 5% ($n = 5$) in the response of four samples demonstrated an excellent reproducibility of the enzymatic method.

And the result revealed that it was an applicable method for organophosphate pesticide-contaminated environmental samples. The high sensitivity combined with excellent selectivity, direct determination, simple and single-step protocol and low cost are the many advantages of the newly developed sensor. In contrast to other biosensors, the present assay did not require sample enrichment of OP compounds from real samples [37,38]. While the applicability of the biosensor has been illustrated for paraoxon, it will also be valid for other pNP-substituted OP pesticides.

4. Conclusions

This paper established a photochemical fluorimetric paraoxon detection method based on enzyme inhibition and fluorescence quenching. The method offered several significant advantages compared with other methods reported. Firstly, the strategy employed DACM to produce the fluorescent signal. Therefore, the background emission was relatively low. Secondly, fluorescence signal decreased when paraoxon was added, and paraoxon could be detected without separating from the solution. Furthermore, the detection limit of the method was low, so it could be used to detect paraoxon sensitively. Finally, this method has been successfully applied for the determination of paraoxon in practical water samples with minimal sample pretreatment. This method achieved quantitative determination of paraoxon ranging from 5.5×10^{-12} mol L^{-1} to 1.8×10^{-10} mol L^{-1}, and provided a detection limit of 3.5×10^{-12} mol L^{-1}, which is comparable to the previously reported enzymatic analysis for paraoxon detection. Enzymatic method based on enzyme inhibition and fluorescence quenching is also useful to detect other OP compounds.

Acknowledgements

This project was supported by the National Natural Science Foundation of China (grant nos. 20775043, 20875056) and the Natural Science Foundation of Shandong Province in China (grant no. Z2008B05).

Appendix A. Supplementary data

Supplementary data associated with this article can be found, in the online version, at doi:10.1016/j.talanta.2011.01.056.

References

[1] Z. Radic, N.A. Pickering, D.C. Vellom, S. Camp, P. Taylor, Biochemistry 32 (1993) 12074–12084.
[2] C. La Rosa, F. Pariente, L. Hernandez, E. Lorenzo, Anal. Chim. Acta 295 (1994) 273–282.
[3] M. Hamada, R. Wintersteiger, JPC 16 (2003) 4–10.
[4] L. Dziri, S. Boussaad, N. Tao, R.M. Leblanc, Langmuir 14 (1998) 4853–4859.
[5] D. Du, J. Wang, J.N. Smith, C. Timchalk, Y. Lin, Anal. Chem. 81 (2009) 9314–9320.
[6] S.M. Hossain, R.E. Luckham, M.J. McFadden, J.D. Brennan, Anal. Chem. 81 (2009) 9055–9064.
[7] C. Zhang, S.V. Malhotra, Talanta 67 (2005) 560–563.
[8] S.D. Aubert, Y. Li, F.M. Raushel, Biochemistry 43 (2004) 5707–5715.
[9] D. Sharma, A. Nagpal, Y.B. Pakade, J.K. Katnoria, Talanta 82 (2010) 1077–1089.
[10] D. Noort, A. Fidder, M.J. van der Schans, A.G. Hulst, Anal. Chem. 78 (2006) 6640–6644.
[11] A. Farran, J. De Pablo, D. Barcelo, J. Chromatogr. 455 (1988) 163–172.
[12] A. Brega, P. Prandini, C. Amaglio, E. Pafumi, J. Chromatogr. 535 (1990) 311–316.
[13] R. Carabias Martinez, E. Rodriguez Gonzalo, M.J. Amigo Moran, J. Hernandez Mendez, J. Chromatogr. 607 (1992) 37–45.
[14] X. Llopis, N. Ibanez-Garcia, S. Alegret, J. Alonso, Anal. Chem. 79 (2007) 3662–3666.
[15] B.J. Privett, J.H. Shin, M.H. Schoenfisch, Anal. Chem. 80 (2008) 4499–4517.
[16] H. Wang, J. Wang, C. Timchalk, Y. Lin, Anal. Chem. 80 (2008) 8477–8484.
[17] C. Wang, X.B. Li, Y.H. Liu, Y.R. Guo, R. Xie, W.J. Gui, G.N. Zhu, J. Agric. Food Chem. 58 (2010) 5658–5663.
[18] E. Mauriz, A. Calle, A. Montoya, L.M. Lechuga, Talanta 69 (2006) 359–364.
[19] C. Dumschat, H. Muller, K. Stein, G. Schwede, Anal. Chim. Acta 252 (1991) 7–9.
[20] J. Orbulescu, C.A. Constantine, V.K. Rastogi, S.S. Shah, J.J. Defrank, R.M. Leblanc, Anal. Chem. 78 (2006) 7016–7021.
[21] H. Schulze, S. Vorlova, F. Villatte, T.T. Bachmann, R.D. Schmid, Biosens. Bioelectron. 18 (2003) 201–209.
[22] Y. Miao, N. He, J.J. Zhu, Chem. Rev. 110 (2010) 5216–5234.
[23] G. Liu, Y. Lin, Anal. Chem. 78 (2006) 835–843.
[24] F. Arduini, F. Ricci, C.S. Tuta, D. Moscone, A. Amine, G. Palleschi, Anal. Chim. Acta 580 (2006) 155–162.
[25] S. Paliwal, M. Wales, T. Good, J. Grimsley, J. Wild, A. Simonian, Anal. Chim. Acta 596 (2007) 9–15.
[26] R. Eickhoff, C. Baldauf, H.W. Koyro, G. Wennemuth, Y. Suga, J. Seitz, R. Henkel, A. Meinhardt, Mol. Hum. Reprod. 10 (2004) 605–611.
[27] I. Smirnova, V. Kasho, J. Sugihara, J.Y. Choe, H.R. Kaback, Biochemistry 48 (2009) 8852–8860.
[28] S. Matsuba, Y. Suga, K. Ishidoh, Y. Hashimoto, K. Takamori, E. Kominami, B. Wilhelm, J. Seitz, H. Ogawa, J. Dermatol. Sci. 30 (2002) 50–62.
[29] R.C. Trievel, F.Y. Li, R. Marmorstein, Anal. Biochem. 287 (2000) 319–328.
[30] P. Kele, J. Orbulescu, T.L. Calhoun, R.M. Leblanc, Langmuir 18 (2002) 8523–8526.

[31] L. Viveros, S. Paliwal, D. McCrae, J. Wild, A. Simonian, Sens. Actuators B 115 (2006) 150–157.
[32] M. Wang, X. Gu, G. Zhang, D. Zhang, D. Zhu, Anal. Chem. 81 (2009) 4444–4449.
[33] A.S. Kalgutkar, B.C. Crews, L.J. Marnett, J. Med. Chem. 39 (1996) 1692–1703.
[34] A.J. Krotzky, B. Zeeh, Pure Appl. Chem. 67 (1995) 2065–2088.
[35] Z. Zou, D. Du, J. Wang, J.N. Smith, C. Timchalk, Y. Li, Y. Lin, Anal. Chem. 82 (2010) 5125–5133.
[36] R.N. Fichorova, N. Richardson-Harman, M. Alfano, L. Belec, C. Carbonneil, S. Chen, L. Cosentino, K. Curtis, C.S. Dezzutti, B. Donoval, G.F. Doncel, M. Donaghay, J.C. Grivel, E. Guzman, M. Hayes, B. Herold, S. Hillier, C. Lackman-Smith, A. Landay, L. Margolis, K.H. Mayer, J.M. Pasicznyk, M. Pallansch-Cokonis, G. Poli, P. Reichelderfer, P. Roberts, I. Rodriguez, H. Saidi, R.R. Sassi, R. Shattock, J.E. Cummins Jr., Anal. Chem. 80 (2008) 4741–4751.
[37] Y.Z. Piao, Y.J. Kim, Y.A. Kim, H.S. Lee, B.D. Hammock, Y.T. Lee, J. Agric. Food Chem. 57 (2009) 10004–10013.
[38] J.Y. Shim, Y.A. Kim, Y.T. Lee, B.D. Hammock, H.S. Lee, J. Agric. Food Chem. 58 (2010) 5241–5247.